A multiproxy approach to characterize the sedimentation of organic carbon in the Amazon continental shelf.

Rodrigo de L. Sobrinho[1,2*], Marcelo C. Bernardes[1], Carlos Eduardo de Rezende[3], Jung-Hyun Kim[2,4], Stefan Schouten[2], Jaap S. Sinninghe Damsté[1,5*]

1 Universidade Federal Fluminense (UFF). Departamento de Geoquímica Ambiental, Niterói RJ, Brazil.

2 NIOZ Royal Netherlands Institute for Sea Research, Department of Marine Microbiology and Biogeochemistry, and Utrecht University, den Burg, the Netherlands.

3 Universidade Estadual do Norte Fluminense (UENF). Laboratório de Ciências Ambientais, Campos dos Goytacazes RJ, Brazil.

4 Korea Polar Research Institute (KOPRI), South Korea

5 Utrecht University, Faculty of Geosciences, Utrecht, The Netherlands

Corresponding authors: limasobrinho@hotmail.com; J.S.SinninghеDamste@uu.nl

Abstract

Surface sediments were collected in a transect from the Amazon river delta to open marine sites in the north Atlantic Ocean in order to characterize spatial contrasts in the deposited organic carbon (OC), allowing to uncover the role of the river plume on the sedimentation of OC. Analysis of isoprenoidal and branched glycerol dialkyl glycerol tetraethers (GDGTs), lignin phenols, fatty acids, *n*-alkanes and bulk parameters were performed to characterize the sedimentary OC. An end member approach based on biomarkers (lignin phenols and GDGTs), and the stable carbon isotopic composition of bulk organic carbon ($\delta^{13}C_{OC}$), was used to estimate the fraction of marine (OC_{mar}) and continental sources (OC_{cont}) of sedimentary organic carbon. Similar estimates based on lignin phenols were obtained and indicates that the OC_{cont} was on average 30 ± 37 %; based on the GDGTs it was 29 ± 35 % while based on the $\delta^{13}C_{OC}$ it was 30 ± 32 %. The OC content of the surface sediments remained relatively constant from the delta to the marine sites northward (ca. 0.6 %) but the fractions of continental and marine OC were variable. In the deltaic region, OC_{cont} was ca. 84%, while in the open marine sites, OC_{mar} was ca. 86%. In the stations southward the delta, the OC content was about 0.03 % with high OC_{mar} and low OC_{cont}, which indicates a low influence of the river plume on this location. The accumulation rates of OC_{cont} and OC_{mar} were estimated and showed that both were higher in the deltaic region in comparison to the marine sites. The results suggested that only 10-15 % of the OC_{cont} is deposited offshore and that river plume conditions stimulated primary production and, thus, ultimately the sedimentation of OC_{mar} in the continental shelf and offshore sediments. Finally, our estimates showed that the Amazon River Delta has an accumulation rate above the global average and the material transported horizontally by the river plume fuels the primary production in adjacent areas, which improves the relevance of the Amazon continental shelf to the global carbon budget.

Keywords: organic carbon, continental organic matter, marine organic matter, biomarkers.

1 Introduction

The burial of organic carbon (OC) in marine sediments is a key process in the global carbon cycle (e.g. Hedges et al., 1997; Liu et al., 2010). Important questions in this respect concern the accumulation rate of organic carbon (AR_{TOC}) and the respective fractions of marine (OC_{mar}) and continental (OC_{cont}) sources of sedimentary organic carbon (SOC) (Berner, 1982; Bianchi et al., 2018; Blair and Aller, 2012; Hedges et al., 1997; Meybeck, 1982). Sediments of deltas and continental shelves are the most important sinks of OC in the present-day oceans (Dagg et al., 2004; McKee et al., 2004). Consequently, many efforts have been made in the last decades to estimate the role of these environments in the global carbon budget (Aller et al., 1996; Burdige, 2005; Galy et al., 2007). In this context, the Amazon River is a major individual contributor of OC_{cont} to the marine environment and, therefore, has been extensively studied (e.g., Aller et al., 1996; Hedges and Keil, 1999; Richey et al., 1990; Schlünz and Schneider, 2000). Due to its magnitude, the burial efficiency of OC calculated in the continental shelf and fan sediments have been used to estimate the global sink of OC in the oceans (Burdige, 2005). The approach to estimate the fractions of OC_{cont} and OC_{mar} in these environments is commonly based on a two-component end-member approach using the stable carbon isotopic composition of the organic matter ($\delta^{13}C_{OC}$) (Aller et al., 1996; Showers and Angle, 1986). However, many processes can affect the values of $\delta^{13}C_{OC}$ in marine sediments. For example, the pre-depositional degradation of organic matter (OM) on land, during transit and in the water column, the input of recycled ancient carbon in continental shelf sediments, and contributions of terrestrial C_4 plants derived detritus with enriched values of $\delta^{13}C$ (-8 to -18 ‰) (e.g. Blair et al., 2003; Goñi et al., 1998; Gordon and Goñi, 2004) can all influence the $\delta^{13}C_{OC}$.

Biomarkers can also be used to assess the contribution of OC_{cont} to the OC in marine sediments. Glycerol dialkyl glycerol tetraethers (GDGTs) are membrane lipids found in the archaeal and bacterial domains of life and are well preserved in sediments (see Schouten et al., 2013 for a

review). They can be applied as biomarkers to trace OC_{cont} input in marine sediments using the BIT Index (cf. Herfort et al., 2006; Hopmans et al., 2004). This proxy is based on the ratio between the sum of branched GDGTs (brGDGTs), derived mainly from the continent, and the isoprenoid GDGT crenarchaeol ($isoGDGT_{cren}$), mainly being produced in the marine environment. The concentrations of these GDGTs have been used to estimate OC_{mar} and OC_{cont} (e.g. Belicka and Harvey, 2009; Herfort et al., 2006; Smith et al., 2010; Weijers et al., 2009). Lignin phenols are alternative biomarkers for tracing OC_{cont}. The lignin macromolecule is a recalcitrant biopolymer produced specifically by vascular plants and is analyzed by the products, lignin phenols, released from CuO oxidation. These CuO oxidation products have been widely applied to trace sources of OC_{cont} to aquatic systems (Bianchi et al., 2007; Goñi and Hedges, 1992; Hedges and Ertel, 1982; Ward et al., 2013). In the marine environment, lignin phenols may be found in pelagic regions, often associated with fine particles, but typically occur in higher concentrations in deltas and the continental shelf, normally associated to coarse particles (Goñi et al., 1998; Hedges and Keil, 1999). The cinamyl and syringyl groups are commonly applied as biomarkers to discriminate woody and non-woody plant material, respectively, transported from the watershed to the ocean. Furthermore, the aldehyde and acid phenols of the vanillin group can be used to identify the degradation state of the SOC (Goñi and Hedges, 1992). Long-chain *n*-alkanes and fatty acids have also been used to trace sources of terrestrial OM to aquatic ecosystems (e.g. Meziane and Tsuchiya, 2000; Mortillaro et al., 2011; Zhu et al., 2013) since they are produced as leaf waxes by higher plants. However, apart from riverine discharge, eolian transport of *n*-alkanes and fatty acids is another important mechanism of transport from continents to marine systems (Schefuß et al., 2003) and the degradation of short chain n-alkanes could also affect the carachteristics of the resilient organic carbon composition. Thus, the interpretation of the results based on these biomarkers must be considered with caution.

Because of the limitations imposed by each biomarker individually, an increasingly number of studies use a multiproxy approach to constrain the input of marine and continental OC in coastal

areas. In this study, we analyzed GDGTs, lignin phenols, fatty acids, *n*-alkanes and bulk parameters in surface sediments of the Amazon continental shelf and marine sites under the influence of the Amazon river plume in order to estimate the contribution of continental OC_{cont} and OC_{mar} to the SOC. The results also provide estimations into the extent to which rates OC is accumulated in the Amazon continental shelf area.

2 Materials and Methods

2.1 Study area

The Amazon basin is the largest drainage area of a river system worldwide (6.2×10^6 km^2) (Molinier et al., 1996). It is mainly covered by tropical forest and wetlands. The Amazon River transfers 1.2×10^9 m^3 y^{-1} of water (Meade et al., 1985) and 3.1×10^{13} g_{OC} y^{-1} of total OC from the continent to the oceans (i.e., 20% of the global input of OC_{cont}) (Richey et al., 1990; Schlünz and Schneider, 2000). Most of the suspended particulate material (SPM) (84%) originates in the Andes. However, the wetlands and the lowland forest also provide significant contribution of OM to the river water (Mayorga et al., 2005; Moreira-Turcq et al., 2004; Moreira-Turcq et al., 2013; Mortillaro et al., 2011; Zell et al., 2013a).

Trade winds are prevalent in the Amazon continental shelf. Its orientation is perpendicular to the coastline and the intensity can vary throughout the year. Semi-diurnal tides also cause currents that are perpendicular to the isobaths (Geyer et al., 1996; Nittrouer and DeMaster, 1996). However, the main force on the direction and speed of dispersion of the river plume is the North Brazil Current (NBC) (Molleri et al., 2010). NBC originates on the south Equatorial Current and flows through the equator and along the continental margin through the Amazon River Delta. It is 100-200km wide and 500m deep (Flagg et al., 1986). The intensity of NBC varies seasonally between 35Sv (July-August) to 10Sv (April-May), with an average of 25Sv (1Sv = 106 m3 / s). The inner-shelf region, under the direct influence of the river plume, extends

for 200 km to the north, becoming narrower near Cabo Cassiporé, where the ANC-5 and ANC-16 stations are located (Fig. 1).

The highest accumulation rates occur between isobates 30-60m (Kuehl et al., 1986). The sediment deposition rate at the Amazon continental shelf has been estimated to be as high as 0.4 - 2.0 cm y^{-1} (Showers and Angle, 1986) and, due to its magnitude, the percentage of OC accumulated in this environment (10%) has been extrapolated to other rivers and used to calculate the global carbon burial budget in the oceans (Burdige, 2005). The sedimentation rates decrease offshore and the grain size also tends to decrease when compared to the delta. Most of the SOC is derived from production in the marine water column and the role of the river plume on the transfer of OC from the delta to the open marine environments is uncertain. The flocculation and the sedimentation of terrestrial material tend to follow the river plume and the NBC (Fig. 1) along the northeast coast (Froidefond et al., 1988; Geyer et al., 2004; Kuehl et al., 1986). From these considerations, it can be concluded that the SPM and sediments along this continent-ocean interface will be very heterogeneous.

Previous studies have proposed to divide the Amazon continental shelf in sub-regions in order to comprehend the geochemical process in this environment. According to Smith and Demaster (1996) the salinity and turbidity in surface waters under the influence of the river plume defines three "zones", which are linked to the primary production in the continental shelf and in the marine sites. Zone I, near the delta, is characteristic of high turbidity (>10 mg L^{-1}) and low salinity (< 2). This area is also found to have a relatively low primary production (8.0 x 10^2 g_{OC} m^{-2} y^{-1}). Zone II is the transition between the delta and marine environment; it is characterized by high primary production (1.0 x 10^3 g_{OC} m^{-2} y^{-1}), as a consequence of the high nutrient availability and lower turbidity (< 10 mg L^{-1}). Zone III, corresponds to open marine environment, with high salinity (> 32) and low turbidity, and a lower primary production (3.7 x 10^2 g_{OC} m^{-2} y^{-1}) due to the lack of nutrients. Diverse regions on the Amazon continental shelf can also be recognized on basis of the sedimentary environment (Kuehl et al., 1986; Smith and

Demaster, 1996), which corresponds to the sediment deposition rates (DR_{sed}) and its sedimentary structures (e.g. clay, mud, etc.).

In the present study we grouped our surface sediments in four regions according to water and sediment characteristics as described in the literature (Showers and Angle, 1986; Fig. 1). Region I lies in the southern part of the continental shelf, where the influence of the Amazon River plume is expected to be lower than the northern site, once it runs northward. The sediments are silty, the DR_{sed} is 0.50 cm y^{-1}. Region II is located in the delta of the Amazon River and directly receives the river discharge. The sediment is predominantly composed of clay, the DR_{sed} is 0.50 cm y^{-1}. Region III is located in the continental shelf approximately 300 km northwards from the river delta. The sediment is composed mostly of clay, the DR_{sed} deposition rate is 0.25 cm y^{-1}. Region IV is located in an open marine setting approximately 1000 km from the delta. The sediment is silty in nature, the DR_{sed} is estimated to be 0.10 cm y^{-1}.

2.2 Sampling

Sampling was performed during the scientific cruise of the ship RV Knorr in the ANACONDAS project in June 2012, when the flux and the plume of the Amazon River was at its maximum (high water season). The transect followed the Amazon River plume from the river mouth to the north Atlantic (Fig. 1). Surface sediment samples were collected on the continental shelf and in the marine environment. The sampling stations are shown in Fig. 1. The surface sediments were collected using a box core which was sliced in 1 cm layers until 5 cm deep. They were immediately freeze-dried on board and transported to the NIOZ laboratory for further analysis.

2.3 Determination of bulk parameters

To determine the bulk parameters (TOC and $\delta^{13}C$), the surface (0-5 cm) sediments were decalcified following the procedure of Hedges and Stern (1984). The 2 mol L^{-1} HCl solution was added to pre-weighed amount of sediment (ca. 0.2 g) of sample and shaken overnight. The pH was then adjusted to 6 - 7. The residue was freeze-dried and weighted. The amount of carbon and nitrogen and the $\delta^{13}C$ value were determined using a Carlo Erba Flash 2000 organic elemental analyzer interfaced with a Thermo Delta V isotope ratio mass spectrometer. The values were calibrated against in-house lab standards which had a reproducibility of ±0.2 ‰.

2.4 Fatty acid and n-alkane analysis

A total lipid extraction was performed using a modified Bligh and Dyer (1959) technique (Pitcher et al., 2009). The total extract was dissolved in dichloromethane (DCM) and diazomethane was added for methylation of fatty acids. The total extract was fractionated using a small column filled with activated aluminum oxide and eluted with *n*-hexane:DCM (1:1, v/v) and DCM in order to obtain the fraction of *n*-alkanes and fatty acids, respectively. The compounds were identified using a Thermo Finnigan Trace DSQ gas chromatograph mass spectrometer (GC-MS) and quantified with an HP 6890 GC system using flame ionization detection (FID). A fused capillary column (50 m x 0.32 mm) coated with CP Sil-5 (film sickness 0.12 µm) was used with helium as carrier gas. For the GC-MS analysis the temperature started at 70^{o}C in injection and increased at rate of 20^{o}C min^{-1} to 130^{o}C and after that at 4^{o}C min^{-1} to 320^{o}C, and then held for 10 min. For the GC/FID, the temperature started at 70^{o}C in injection and increased at rate of 20^{o}C min^{-1} to 200^{o}C and then for 3^{o}C min^{-1} to 320^{o}C, which was held for 30 min. The scan range used for the GC/MS analysis was 50-800m/z

2.5 Lignin phenol analysis

Freeze-dried sediments were analyzed for lignin monomers using the alkaline CuO oxidation method (Hedges and Ertel, 1982). Briefly, the sediment samples (ca. 500 mg) were transferred to stainless steel reaction vials and digested with 300 mg CuO in 2 mol L^{-1} NaOH solution under N_2 in an oxygen-free atmosphere at 150°C for 150 min. The samples were acidified to pH 1-3 and subsequently 6 mL of ethyl acetate was added. After centrifuging at 2500 rpm for 5 min, the supernatant was collected, dried with sodium sulfate (Na_2SO_4), evaporated under a stream of N_2, redissolved in pyridine, and converted to trimethylsilyl derivatives using bis-(trimethylsilyl) trifluoroacetamide (BSTFA) at 60ºC for 20 min. Oxidation products were analyzed using an HP Agilent 6890N Series gas chromatograph coupled to a flame ionization detector (FID). A fused capillary column (50 m x 0.32 mm) coated with CP Sil-5 (film sickness 0.12 µm) was used with helium as carrier gas. The temperature started at 100ºC in injection and then increased to 150ºC at rate of 4ºC min^{-1}, after that it increased to 215ºC at rate of 5ºC and finally increased to 300ºC at rate of 10ºC and held for 10min. The scan range used for the GC/MS analysis was 50-800m/z The recovery factor was calculated using the surrogate standard ethyl vanillin added prior to analysis (samples with recovery values above 60% were considered). Response factors were determined using a mixture of commercial standards, containing all the lignin phenols analysed in four different concentrations (10 µg ml^{-1}, 7,5 µg ml^{-1}, 5 µg ml^{-1}, 2,5 µg ml^{-1}) which were periodically injected for calibration.

Phenol concentrations are reported as the OC-normalized sum of eight lignin-derived reaction products (λ8 mg g_{oc}^{-1}), including vanillyl (V-series) phenols (vanillin, acetovanillone, and vanillic acid), syringyl (S-series) phenols (syringealdehyde, acetosyringone, and syringic acid), and cinnamyl (C-series) phenols (cumaric acid and ferulic acid). The S:V and C:V ratios were calculated to identify angiosperm tissue sources. The ratio of acidic to aldehyde vanillyl phenols ((Ad:Al)v) was used as an indicator of the lignin degradation state (Hedges and Ertel, 1982).

2.6 Analysis of GDGTs

The freeze-dried samples were extracted with a modified Bligh and Dyer (1959) technique (Pitcher et al., 2009). The total lipid extracts (TLEs) were fractionated in core lipid (CL) fractions using column chromatography (Pitcher et al., 2009). Analyses were performed as described by Hopmans et al. (2000) and Schouten et al. (2007) using an Agilent (Palo Alto, CA) 1100 series LC-MSD SL equipped with an autoinjector and Chemstation software. The injection volume was 10 □l. The flow rate was 0.2 ml/min. After each analysis the column was cleaned by back-flushing it with *n*-hexane–isopropanol (90:10, vol/vol). Compounds in the eluent were detected using atmospheric pressure positive-ion chemical ionization (APCI)-MS. GDGTs were detected by mass scanning from *m/z* 950 to 1450 and quantified by integration of the peak areas of their $[M□H]^{□}$ and $[M□H□1]^{□}$ ions as reported by Schouten et al. (2008). Quantification of the GDGTs was achieved by integrating the peak areas and using a C_{46} GDGT internal standard following the procedure of Huguet et al. (2006).

2.7 Statistics

Data set of each parameter showed no normal distribution thus, non-parametric Kruskal-Wallis tests were performed to compare means. The *p*-values lower than 5% were considered as significant differences between the compared means. Statistical analyzes, bar graphs and boxplots were performed using the R program (version 3.3.3). For the statistical analyzes it was used the Stats package and for the graphs it was used the ggplo2 and cowplot packages.

3 Results

3.1 Bulk parameters

The OC content of the sediments (Fig. 2A) shows an overall average value of 0.6 ± 0.4 wt.%. The maximum value was found on station ANC-5 (1.1%) located in the continental shelf NW

from the river mouth and the lowest value on station ANC-13 (<0.1%) located in SE from the river mouth (Fig 1). The bulk $\delta^{13}C_{OC}$ varies from -20.3 and -20.7‰ in region IV at stations ANC-1 and 2, respectively, to -27.3 and -26.8‰ in region II at stations ANC-10 and 11, respectively (Fig. 2B, Table 1).

3.2 Branched and Isoprenoid GDGTs

The highest concentrations of brGDGTs are observed in region II (Fig. 2C) with values of 56.6 µg g_{OC}^{-1} in sample ANC-10 and 31.1 µg g_{OC}^{-1} in sample ANC-11 (Table 1). The lowest values are found in region IV, where stations ANC-1 and ANC-2 have concentrations of 3.9 and 5.7 µg g_{OC}^{1}, respectively. The concentration of crenarchaeol is highest at station ANC-14 (159.6 µg g_{OC}^{-1}) and its lowest concentration is observed in the deltaic station ANC-11 (28.7 µg g_{OC}^{-1}) (Fig. 2D, Table 1). Most of the surface sediments have values for the BIT-index of <0.5 (Fig. 2E). Exceptions are the deltaic stations (region II) ANC-10 (0.57) and ANC-11 (0.52). In the open marine environment (region IV), the values of the BIT-index in the stations ANC-1 and 2 are <0.1.

3.3. Lignin Phenols

The concentrations of lignin-derived phenols are highest in the stations located in region II (Fig. 2F) with values for λ8 of 41.2 mg g_{OC}^{-1} in station ANC-10 and 13.3 mg g_{OC}^{-1} in station ANC11 (Table 1). The lowest values for λ8 are found in stations ANC-1 and ANC-2 (0.2 mg g_{OC}^{-1}). The S:V ratio shows similar values along the transect from region I to III, varying between 0.5 and 0.8. In region IV these values are relatively lower (0.3 and 0.4). The C:V values are low at all stations with the highest value (0.24) for station ANC-1. The (Ad:Al)v values are also constant along the transect from the delta to the marine site, with values between 0.1-0.3 (Table 1).

3.4 Fatty acids and n-Alkanes

The fatty acids in sediments mainly comprised C_{14} – C_{32} saturated fatty acids. Furthermore, also *iso* and *anteiso* 15, 16:1, *iso* 16, 18:1, C_{10} – C_{18} fatty acids and ββ-C_{32} hopanoic acid was identified. The highest concentration of total fatty acids (Σ_{FA}) are found in region I, where the samples ANC-14 and ANC-13 have values of 6.1 and 5.5 mg g_{OC}^{-1} respectively (Fig. 2G, Table 1). The lowest values are observed in region IV, where the concentrations of fatty acids are 0.9 mg g_{OC}^{-1} in sample ANC-1 and 1.1 mg g_{OC}^{-1} in sample ANC-2. The highest concentrations of long-chain fatty acids (LCFA; >C_{24}) were found in region II (Fig. 2H, Table 1). The LCFA concentrations for samples ANC10 and ANC-11 are 1.9 and 2.0 mg g_{OC}^{-1}, respectively. The C_{20}-C_{30} LCFA showed an even-over-odd carbon number predominance varying between 1.3 in sample ANC-11 to 4.4 in sample ANC-14 (Table 1). No clear differences between the four regions are observed for this parameter.

The highest concentration of long-chain *n*-alkanes with an odd number of carbon atoms (C_{27-33}) is found in region I (Fig. 2I), where the concentrations for samples ANC-13 and ANC-14 are 0.4 and 0.7 mg g_{OC}^{-1}, respectively (Table 2I). The lowest values of C_{27-33} are observed in region IV, where the concentration on stations ANC-1 and ANC-2 is 0.1 mg g_{OC}^{-1}. The Carbon Preference Index (CPI) show values higher then 1.0 in all samples. On station ANC-2 is observed the highest value of CPI (2.4) and the lowest value is observed on station ANC-13 (1.5).

4 Discussion

4.1 Sources of sedimentary organic carbon

Substantial changes in TOC content were observed in surface sediments in the spatial transect (Fig. 2a). The concentrations of brGDGTs, λ8, LCFAs, i.e. biomarkers to trace OC_{cont}, revealed a similar trend from the delta to the open ocean sites with maximum concentrations in the delta

(region II) (Fig. 2C, and 2F). The concentrations of $C_{27\text{-}31}$ *n*-alkanes also decrease offshore, however the highest concentrations were observed in region I (Fig. 2I). It corroborates previous studies in the Amazon continental shelf and other estuaries, which showed that the delta is the principal sector for the sedimentation of OC_{cont} (e.g. Aller et al., 1996; Burdige, 2005; Cui et al., 2016; Hedges et al., 1997; Sinninghe Damsté, 2016). These results also suggest that OC_{mar} is the primary source of sedimentary OC in region IV as there brGDGTs, λ8, LCFAs and long-chain *n*-alkanes have minimal values. This interpretation is reinforced by the results of $\delta^{13}C_{OC}$ and BIT-Index (Fig. 2B and 2E). The values of $\delta^{13}C_{OC}$ in region IV were close to typical values for marine OM (-19.0‰) (Foges and Cifuentes, 1993; Hedges et al., 1997) and the values of BIT-Index were much lower (i.e. <0.1; typical for open marine environments; Schouten et al., 2013) in regions III and IV than in region II (>0.5). Thus, both parameters indicate a stronger contribution of marine sources to the sedimentary OC offshore.

Lignin phenols showed that the S:V and C:V ratios maintained their respective values throughout the transect. S:V values ranged from 0.32 to 0.82, while C:V values ranged from 0.03 to 0.24 These results indicate that the sedimented continental plant material is composed mainly of angiosperms woods and leaves (Goñi et al., 1998; Hedges et al., 1986) and the composition of lignin phenols in the sediment originates mainly from the forest soil drainage and does not change significantly along its horizontal transport. In addition, the values of (Ad:Al)v showed little variation between samples collected in the delta and those collected offshore, with values indicating partially degraded material (Ertel and Hedges, 1985). This observation shows that lignin molecules have a recalcitrant characteristic and did not undergo degradation after deposition on the surface sediment. This observation reinforces that lignin phenols can be used as biomarkers to trace changes in plant coverture in paleoclimatic reconstruction studies (Sun et al., 2017).

Although diverse parameters reinforce that the majority of OC_{cont} is deposited in the deltaic region, the absolute values of individual parameters cannot be used directly to quantify the

relative fractions of OC_{cont} and OC_{mar}. Furthermore, some may also be affected by different factors which complicate their use to quantitatively estimate the contribution of OC_{cont} to SOC. For example, eolian transport can significantly affect the concentration of fatty acids and *n*-alkanes in marine sediments (Schefuß et al., 2003). Moreover, it is not possible to quantify the contribution of wind transport to the composition of the SOC based on present data. Thus, we applied three two-component mixing models based on a bulk parameter ($\delta^{13}C_{OC}$) and two biomarker classes (BIT index and λ8), respectively, in order to estimate the continental and marine sources to sedimentary OC (OC_{cont} and OC_{mar}). Each estimation is associated with various complicating factors (Zhu et al., 2013). For example, the continental end-member of $\delta^{13}C_{OC}$ may be biased because higher plant material may also (partly) derive from C_4 plants that have higher $\delta^{13}C$ values than C_3 plants (e.g. Blair et al., 2003; Goñi et al., 1998; Gordon and Goñi, 2004). The BIT Index *in situ* production of brGDGTs in marine sediments complicates the application of this proxy though typically this does not lead to a large effect on the BIT index (Sinninghe Damsté, 2016). However, the production of crenarchaeol has been observed in river systems (De Jonge et al., 2015) decreasing the BIT index. Indeed, the river and floodplain lakes have been reported as sources of crenarchaeol production in the Amazon river system (Zell et al., 2013b). Lignin phenols, on the other hand, are highly specific for continental OM sources (woody and non-wood plants) and can be found in buried marine sediments in relatively high concentrations when compared to other organic molecules (Goñi et al., 1998). Hence, lignin is relatively recalcitrant, even though, lignin degradation can be an important source of outgassing CO_2 in the Amazon basin (Ward et al., 2013).

We used equations 1-3 to estimate the continental fraction of the SOC. As the continental endmember values for the proxies BIT and, λ8, the average values reported for the Amazon River (Table 2) were used. The marine end member value for the $\delta^{13}C_{OC}$ was chosen according to data reported in the literature (Burdige, 2005), the marine end member for the BIT was chosen as 0.04 (Schouten et al., 2013) and the marine end member for λ8 was null (Table 2). The marine

fraction was estimated based on the difference between the total OC and its continental fraction (OC_{cont}) (Eq. 4).

$$OC_{cont}(\delta^{13}C) = \frac{(\delta^{13}C_{sed} - \delta^{13}C_{mar})}{(\delta^{13}C_{cont} - \delta^{13}C_{mar})} \text{ x } 100 \quad \text{(Eq. 1)}$$

$$OC_{cont}(\text{BIT Index}) = \frac{(BIT_{sed} - BIT_{mar})}{(BIT_{cont} - BIT_{mar})} \text{ x } 100 \quad \text{(Eq. 2)}$$

$$OC_{cont}(\lambda 8) = \frac{\lambda 8_{sed}}{\lambda 8_{cont}} \text{ x } 100 \quad \text{(Eq. 3)}$$

$$OC_{cont}(100\%) = OC_{mar}\ (\%) + OC_{cont}\ (\%) \quad \text{(Eq. 4)}$$

$$\Delta\, OC_{cont} = \frac{OC_{cont\,(\alpha)} - \mu OC_{cont}}{\mu OC_{cont}} \text{ x } 100 \quad \text{(Eq. 5)}$$

Although the proxies vary in their physical-chemical characteristics and in their sources, the estimations of the OC_{cont} based on each parameter were similar (Fig. 3A and 3B). In order to calculate any possible differences between the estimations of each proxy, the values of OC_{cont} obtained by equations 1 – 3 of a sampling site was subtracted by the average value of this parameter in the respective station and normalized by percentage according to equation 5. In this equation $OC_{cont\,(\alpha)}$ refers to the percentage of OC_{cont} estimated by a parameter (α) and μOC_{cont} is the mean of the estimations of the three parameters in the respective station. Thus, the average values of this calculation are presented in Fig. 4. According to this approach, the estimations of OC_{cont} based on lignin phenols, the BIT index and the $\delta^{13}C$ showed no significant difference with each other (p = 0.52). Further, the results of OC_{cont} provided by the different proxies, showed good correlation (r_s = 0.82 for $\delta^{13}C$ vs. $\lambda 8$, r_s = 0.97 for BIT vs. $\lambda 8$ and r_s = 0.88 for $\delta^{13}C$ vs. BIT; n = 8).

The OC_{cont} estimated by these three approaches showed a substantial spatial variation along the studied transect (Figs. 3A). It was highest ($p < 0.01$) in Region II (stations ANC-10 and ANC-11) based on all proxies (Fig. 3B). In this region, the highest OC_{cont} was estimated by the BIT index in station ANC-10 (85 %) and the lowest OC_{cont} by the λ8, in station ANC-11 (74 %). In the ANC-10 sample, the lignin concentration measured in the sediment was higher than the reference value for that region. Thus, in this case, the OC_{cont} fraction was considered as 100% (Figs. 3A). In the open marine environment (region IV) OC_{cont} showed a much wider range of values compared to the other regions. The highest percentage of OC_{cont} was estimated by the $\delta^{13}C$ in sediment ANC-2 (7 %) and the lowest by the λ8 proxy in sediments ANC-1 and ANC-2 (1 %). The average percentage of OC_{cont} in region II was 80 ± 11 %, while in region IV the percentage of the OC_{mar} was 97 ± 2 %. The fractions of OC_{cont} and OC_{mar} calculated by these equations corroborate the estimations based on the $\delta^{13}C$ end member approach performed by Aller et al. (1986), according to which the fractions of OC_{cont} and OC_{mar} in the delta of the Amazon river were 70 and 30 %, respectively. This reinforces that the sedimentation of OC_{cont} transported by the Amazon river occurs predominantly in the delta and, due to the re-mineralization and burial of the OM, only a minor part (10 – 15%) of the OC_{cont} discharged by the river into the ocean reaches the sediments offshore. Estimates based on the combination of three proxies, although performed on a limited number of samples, supports the outcome of the studies previously performed in this area to estimate OC_{cont} (Aller et al., 1996, Kuehl et al., 1986, Sun et al., 2017).

4.2 Accumulation of continental and marine organic carbon transection in the Amazon Shelf

The accumulation rate of continental organic carbon (AR_{cont}) and marine organic carbon (AR_{mar}) can be estimated if the accumulation rate of OC (AR_{TOC}), the particle dry density and sediment porosity are known. In order to quantify AR_{cont} and AR_{mar}, we followed previously

applied methods to estimate the AR_{TOC} (Showers and Angle, 1986). To estimate a real accumulation, we must integrate the particle dry density, porosity and DR_{sed} in each region as presented in equation 6. Values for the particle dry density, porosity, and DR_{sed} were based on literature data (Table 2). Subsequently, the AR_{cont} and AR_{mar} were estimated according to equations 7 and 8.

$$\mathrm{AR_{TOC}\ (g\ m^{-2}\ y^{-1}\ )} = \frac{\mathrm{Part.\ Dens.\ (g\ cm^{-3}\ )\ x\ (1-porosity)x\ DR_{sed}\ x\ TOC(\%)}}{100} \quad \text{(Eq. 6)}$$

$$\mathrm{AR_{cont}\ (g_{OC}\ m^{-2}\ y^{-1}\ )} = \frac{\mathrm{AR_{TOC}\ x\ OC_{cont}\ (\%)}}{100} \quad \text{(Eq. 7)}$$

$$AR_{TOC} = AR_{mar} + AR_{cont} \quad \text{(Eq. 8)}$$

The proposed model ignores other processes such as resuspension, and bioturbation, which could stimulate the remineralization of the sedimentary OC. Consequently, our approach likely provides an overestimate of OC accumulation rates. Another relevant aspect to be considered is that the mean values used to calculate the mixing models and the sediment accumulation have quite some variation, even within one zone (Table 1). In addition, the flux in the Amazon river and the direction of the river plume changes radically over the hydrological seasons, due to the periodic floods and the marine currents (Coles et al., 2015; Molleri, et al., 2010; Prestesa et al., 2018). Thus, our results did not include all the events and processes that could affect the quantification of carbon burial in the continental shelf and marine sites. However, our results could inform further studies in this environment and other deltaic and river plume settings. On the Amazon continental shelf, there is a large data base related to sediment accumulations rates, sediment density and porosity (Kuehl, 1982; Reymond and Bauer, 2001; Smith and Demaster, 1996) which allows the application of our multiproxy approach. However, to increase the accuracy the sampling density should increase and all data should be collected and processed using the same approach. Besides, the organic matter characterization underlying AR_{TOC}

estimation should be done at the same site and during the same period as the sediment depositional data collection.

The estimations of AR_{TOC} for each region varied from 1 g_{OC} m^{-2} y^{-1} in station ANC-13 to 30 g_{OC} m^{-2} y^{-1} in station 11 (Fig. 5A). Region II showed by far the highest values of AR_{cont} (20 ± 4 g_{OC} m^{-2} y^{-1}; Fig. 5B). The other regions were characterized by significantly ($p < 0.01$) lower values. With respect to AR_{mar}, region II and III have higher average values (6 ± 2 g_{OC} m^{-2} y^{-1} and 9 ± 8 g_{OC} m^{-2} y^{1} respectively; Fig. 5C). Thus, even though region II has the lowest percentages of OC_{mar}, the AR_{mar} is rather high (Fig. 6). This can be explained by the interaction between the material produced in the water column and the particulate material discharged by the river, which increases the sedimentation rate of both marine and continental OC in that region. The opposite condition is observed in region I and IV where the fraction of OC_{mar} in the sediment is high but the AR_{mar} is low. In these areas the sediment deposition rate is low and consequently the AR_{cont} and AR_{mar} are lower than the delta. In region III, a high percentage of OC_{mar} is observed and also AR_{mar} is also high (Fig. 6). This region at the interface between high primary production and sediment accumulation zones has sediments with a high percentage of OC_{mar} and high AR_{mar}. The wide range of values (Fig. 5C) observed in this region can also be explained as a consequence of the location of the two sampling sites (ANC-5 and ANC16). Both are located at similar latitudes, however, the first is near the coast line, whereas the second is located on the continental slope. Different depths can affect the sedimentation of CO as a result of microbial metabolism in the water column and the fragmentation of particulate material (Briggs et al., 2019; Nayak and Twardowski, 2020). Therefore, the difference in depth between the ANC-5 and ANC-16 stations may also explain the differences observed between these two stations.

The flocculation of the material transported by the river as well as its horizontal transport is mainly related to the particle size, being larger particles more easily precipitated and with lower potential for horizontal displacement. Factors related to mineral particle size are salinity and

composition of organic matter adsorbed to the suspended sediment. This is because mineral particles are more easily precipitated in saline waters than freshwater (e.g., Kranck, 1980; Krone, 1962;Whitehouse et al., 1960;) and the molecular composition of OC can increase the adhesion between mineral particles and thereby promoting flocculation (Eisma et al., 1991; O'Melia and Tiller, 1993). In the case of the Amazon River, the material discharged into the Atlantic Ocean is predominantly composed of fine particles, which allows greater fluctuation (e.g. Hedges et al., 1986; Ward et al., 2015). The high river flow enables freshwater intrusion into the marine ecosystem throughout the year and this material is predominantly transported in the NW direction (Coles et al., 2013). Thus, suspended particulate organic carbon (SPOC) flocculation tends to occur on the continental shelf. The shallow depth of the continental shelf near the delta and tidal variations produce an intense mixing zone that extends up to 150 km along the shoreline (Geyer and Kineke, 1995). The intense mixture of suspended sediment keeps the water column turbid without stratification along the mixing zone (Curtin and Legeckis, 1986; Walker and Hammack, 2000; Wright et al., 1986). According to our observations, region II which is characterized by a high energy mixing zone, favors the sedimentation of OC, and corroborates what was presented by Jaeger and Nittrouer (1995) and Kuehl et al. (1996).

The frontal zone of the Amazon River plume is located about 150 km away from the delta and is approximately 50 km long (Geyer et al., 2004). In this region the water column is stratified and the suspended material out of contact with the sediment. The frontal zone tends to favor the precipitation of particulate material and the sedimented material suffers less resuspension when compared to the deltaic region. Particularly in the Amazon River plume, the precipitated material is very dense and suffers little horizontal transport. At the same time, strong downwelling-favorable winds cause the plume to narrow and remain close to the shoreline (Berdeal et al., 2002). Region III would therefore be strongly influenced by the processes occurring in the frontal zone. In this region, the ANC-5 station is under greater influence of the river plume and therefore presents higher percentages of the continental OC fraction and higher sedimentation rates

(AR_{TOC} Fig. 5a). In contrast, the ANC-16 station has lower absolute TOC values as well as low OC_{mar} percentage and AR_{TOC}, suggesting that the river plume has no influence at this station.

As noted earlier, the composition of OC between regions II and IV is significantly different, however the TOC content does not show a clear difference. At the same time, in region I where OC_{mar} prevails, as well as in region IV, the TOC content is low. This suggests that the difference between the TOC content between regions I and IV is due to the presence of particulate and / or dissolved material carried by the river plume to region IV, which would stimulate autochthonous production as well as flocculation (Ahlgren et al., 1992; Medeiros et al., 2012; 2015; Seidel et al., 2015). Interestingly, the estimations of OC_{cont} and OC_{mar} for the dissolved organic carbon (DOC) in these same regions are very similar to what was estimated for the SOC (Seidel et al., 2015). However, more data should be produced to compare the organic composition of the SPOC, DOC and SOC. Based on these observations, it can be concluded that the river plume is determinant for the horizontal and vertical transport of SPM in the continental shelf and consequently defines which regions of the continental shelf present more accurate records about the vegetation cover of the drainage basin. Stations in areas of indirect influence, such as region IV and I and station ANC-16, tend to record more information about marine biogeochemical processes. Finally, the values of AR_{cont} estimated for the deltaic region of the Amazon river is ten times higher than global average (2.6 g_{OC} m^{-2} yr^{-1}) for these environments (Cui et al., 2016 and references within). On the other hand, the estimations of AR_{cont} in the continental shelf and in the marine site are similar to the global average (Cui et al., 2016 and references within). Thus, Amazon continental shelf sediments have similar concentrations of TOC and AR_{TOC} as other shelf regions around the globe, as discussed above. However, the Amazon river plume fuels the primary production in an extensive area in the Atlantic, which affect the sedimentation of OC_{mar} and promotes high accumulation rate of the OC derived from this source in the continental shelf and in adjacent marine sites.

5 Conclusions

The application of stable carbon isotopes and biomarkers, namely GDGTs and lignin phenols, based on an end-members approach, made it possible to estimate OC_{cont} and OC_{mar} fractions of SOC as well as their respective accumulation rates with statistical accuracy. Even considering the small number of samples in a large-scale sample set (aprox. 1,000 km), the results corroborate what was previously reported about the SOC in the Amazon continental shelf. The composition of lignin phenols showed little variation between what was sedimented in the delta and what was sedimented offshore. Thus, lignin phenols are biomarkers that can be applied to trace the composition of the vegetation cover of the drainage basin, even if collected in distant regions of the delta and in marine sediments. In region II (delta) and region IV (marine) the concentration of TOC is similar, however the OC_{cont} and OC_{mar} fractions are quite variable. In the delta, most of SOC is composed by OC_{cont} and only a small fraction is transported to more distant locations on the continental shelf and marine sites. In what concerns to the accumulation rates, the highest values were obtained near the plume frontal zone where well mixed and turbid waters are found. In addition, the OC_{mar} fractions observed in the sediment samples are similar to those reported for dissolved material in these same regions. These observations point to the role of the river plume on primary production and flocculation of particulate and dissolved material. Thus, the deltaic region of the Amazon River sediments OC above the global average and fuels primary production in adjacent areas. As a consequente, the continental shelf and marine sites under the influence of the river plume are determinant for estimating the global carbon budget.

Acknowledgements

RLS and MCB thank the fellows from CAPES, CNPq (245523/2012-0 and 308535/2016-2) and

FAPERJ (E-26/202.796/2016) and the support from CAPES 01 (PPG-Geoquímica-UFF), CNPq (457018/2014-3) and CLIMATE-PRINT-UFF (88887.310301/2018-00). The authors thank the crew of R/V Knorr ship from Woods Hole Oceanographic Institution and Anacondas project through its funding Agency: The Gordon and Betty Moore Foundation #2293 and NSF #OCE-0934095. The work was further supported by funding from the Netherlands Earth System Science Center (NESSC) through a gravitation grant (NWO 024.002.001) from the Dutch Ministry for Education, Culture and Science to JSSD.

References

Aller, R.C., Blair, N.E., Xia, Q. and Rude, P.D., 1996. Remineralization rates, recycling, and storage of carbon in Amazon shelf sediments. Continental Shelf Research 16, 753-786.

Ahlgren, G., I. B. Gustafsson, M. Boberg, 1992. Fatty acid content and chemical composition of freshwater microalgae, Journal of Phycology, 28, 37–50.

Belicka, L.L., Harvey, H.R., 2009. The sequestration of terrestrial organic carbon in Arctic Ocean sediments: A comparison of methods and implications for regional carbon budgets. Geochimica et Cosmochimica Acta 73, 6231 – 6248.

Berdeal, I.G., Hickey, B.M., Kawase, M., 2002. Influence of wind stress and ambient flow on a high discharge river plume. Journal Geophysical Research 107 (C9), 3130.

Berner, R.A., 1982. Burial of organic carbon and pyrite sulfur in the modern ocean: Its geochemical and environmental significance. American Journal of Science 282, 451-473.

Bianchi, T.S., Galler, J.J., Allison, M.A., 2007. Hydrodynamic sorting and transport of terrestrially derived organic carbon in sediments of the Mississippi and Atchafalaya rivers. Estuarine, Coastal and Shelf Science 73, 211-222.

Bianchi T.S., Cui X., Blair N.E., Burdige D.J., Eglinton T.I., Galy V., 2018. Centers of organic carbon burial and oxidation at the land-ocean interface. Organic Geochemistry. 115, 138–155.

Blair, N.E., Leithold, E.L., Ford S.T., Peeler, K.A., Holmes, J.C., Perkey D.W., 2003. The persistence of memory: The fate of ancient sedimentary organic carbon in a modern sedimentary system. Geochimica et Cosmochimica Acta 67, 63–73.

Blair, N.E., Aller R.C., 2012. The fate of terrestrial organic carbon in the marine environment. Annual Review of Marine Science 4, 401-423.

Bligh, E.G., Dyer, W.J., 1959. A rapid method of total lipid extraction and purification. Canadian Journal of Biochemistry and Physiology 37, 911-917.

Briggs N., Dall'Olmo G., Claustre H., 2019. Major role of particle fragmentation in regulating biological sequestration of CO_2 by the oceans. Science 367, 791–793.

Burdige, D.J., 2005. Burial of terrestrial organic matter in marine sediments: A re-assessment. Global Biogeochemical Cycles 19, 1-7.

Coles V.J., Brooks M.T., Hopkins J., Stukel M.R., Yager P.L., Hood R.R., 2013. The pathways and properties of the Amazon River Plume in the tropical North Atlantic Ocean. Journal of Feophysical Research: Oceans, 118, 6894-6913.

Coles V.J., Brooks M.T., Hopkins J., Stukel M.R., Yager P.L., Hood R.R., 2015. The pathways and properties of the Amazon River Plume in the tropical North Atlantic Ocean. Journal of Geophysical Research: Oceans. 118, 6894–6913.

Cui X., Bianchi T.S., Savage C., Smith R.W., 2016. Organic carbon burial in fjords: Terrestrial versus marine inputs. Earth and Planetary Science Letters 451, 41–50.

Curtin, T.B., Legeckis, R.V., 1986. Physical observations in the plume region of the Amazon River during peak discharge— I. surface variability. Continental Shelf Research 6 (1–2), 31–51.

Dagg, M., Benner, R., Lohrenz S., Lawrence, D., 2004. Transformation of dissolved and particulate materials on continental shelves influenced by large rivers: plume processes. Continental Shelf Research 24, 833–858.

De Jonge, C., Stadnitskaia, A., Fedotov, A., Damsté, J.S.S., 2015. Impact of riverine suspended particulate matter on the branched glycerol dialkyl glycerol tetraether composition of lakes: The outflow of the Selenga River in Lake Baikal (Russia). Organic Geochemistry 83–84, 241–252.

Eisma, D., Bernard, P., Cadee, G.C., Ittekkot, V., Kalf, J., Laane, R., Martin, J.M., Mook, W.G., van Put, A., Schuhmacher, T., 1991. Suspended-matter particle size in some West-European estuaries; Part II: A review of floc formation and break-up. Netherlands Journal of Sea Research 28, 215– 220.

Ertel, J.R., Hedges, J.I., 1985. Sources of sedimentary humic substances: vascular plant debris, Geochimica Cosmochimica Acta, 49, 2097–2107.

Fogel, M.L., Cifuentes, L.A., 1993. Isotope fractionation during primary production, in Organic Geochemistry, edited by S. A. Macko and M. H. Engel, pp. 73–98, Springer, New York.

Froidefond, J.M., Pujos, M., Andre, X., 1988. Migration of mud banks and changing coast line in French Guiana. Marine Geology 84, 19-30.

Galy, V., France-Lanord, C., Beyssac, O., Faure, P., Kudrass, H., Palhol, F., 2007. Efficient organic carbon burial in the Bengal fan sustained by the Himalayan erosional system. Nature 450, 407411.

Geyer, W.R., Kineke, G.C., 1995. Observations of currents and water properties in the Amazon frontal zone. Journal of Geophysical Research 100, 2321–2339.

Geyer W.R., Beardsley R.C, Lentz S.J., Candela J., Limeburner R., Johns W.E., Castro B.M., Soares I.D., 1996. Physical ocenography of the Amazon shelf, Continental Shelf Research, 16, 5/6, 575-616.

Geyer W.R., Hill P.S., Kineke, G.C., 2004. The transport, transformation and dispersal of sediment by buoyant coastal flows. Continental Shelf Research 24, 927–949.

Goñi, M.A., Hedges, J.I., 1992. Lignin Dimers - Structures, Distribution, and Potential Geochemical Applications. Geochimica et Cosmochimica Acta 56, 4025-4043.

Goñi, M.A., Ruttenberg, K.C., Eglinton, T.I., 1998. A reassessment of the sources and importance of land-derived organic matter in surface sediments from the Gulf of Mexico. Geochimica et Cosmochimica Acta 62, 3055-3075.

Gordon, E.S., andGoñi, M.A., 2004. Controls on the distribution of and accumulation of terrigenous organic matter in sediments from the Mississippi and Atchafalaya river margins, Marine Chemistry 92, 331–352.

Hedges, J.I., Ertel, J.R., 1982. Characterization of lignin by gas capillary chromatography of cupric oxide oxidation products. Analytical Chemistry 54, 174-178.

Hedges, J.I., Stern, J.H., 1984. Carbon and Nitrogen Determinations of Carbonate-Containing Solids. Limnology and Oceanography. 29, 657-663.

Hedges, J.I., Clark, W.A., Quay, P.D., Richey, J.E., Devol, A.H., andSantos, U.M., 1986. Compositions and fluxes of particulate organic material in the Amazon River, Limnology Oceanography, 31, 717–738.

Hedges, J.I., Keil, R.G., Benner, R., 1997. What happens to terrestrial organic matter in the ocean? Organic Geochemistry 27, 195-212.

Hedges, J.I., andKeil, R.G., 1999. Organic geochemical perspectives on estuarine processes: sorption reactions and consequences. Marine Chemistry 65, 55-65.

Herfort, L., Schouten, S., Boon, J.P., Woltering, M., Baas, M., Weijers, J.W.H., Sinninghe Damsté, J.S., 2006. Characterization of Transport and Deposition of Terrestrial Organic Matter in the Southern North Sea Using the BIT Index. Limnology and Oceanography 51, 2196-2205.

Hopmans, E. C., S. Schouten, R. D. Pancost, M. T. J. van der Meer, and J. S. Sinninghe Damsté. 2000. Analysis of intact tetraether lipids in archaeal cell material and sediments by high performance liquid chromatography/atmo- spheric pressure chemical ionization mass spectrometry. Rapid Commun. Mass Spectrom. 14:585–589.

Hopmans, E.C., Weijers, J.W.H., Schefuß, E., Herfort, L., Sinninghe Damsté, J.S., Schouten, S., 2004. A novel proxy for terrestrial organic matter in sediments based on branched and isoprenoid tetraether lipids. Earth and Planetary Science Letters 224, 107-116.

Huguet, C., Hopmans, E.C., Febo-Ayala, W., Thompson, D.H., Sinninghe Damsté, J.S., Schouten, S., 2006. An improved method to determine the absolute abundance of glycerol dibiphytanyl glycerol tetraether lipids. Organic Geochemistry 37, 1036-1041.

Jaeger, J.M., Nittrouer, C.A., 1995. Tidal controls on the formation of fine-scale sedimentary strata near the Amazon river Mouth. Marine Geology 125, 259–281.

Kranck, K., 1980. Experiments on the significance of floccula-tion in the settling of fine-rained sediment in still water. Canadian Journal of Earth Sciences 17, 1517–1526.

Krone, R.B., 1962. Flume Studies of the Transport of Sediment in Estuarial Shoaling Processes. Hydraulic Engineering and Sanitary Engineering Research Laboratory, University of California, Berkeley, 1–110.

Kuehl, S.A., Nittrouer C.A., DeMaster D.J., 1982. Modern sediment accumulation and trata formato on the Amazon continental shelf. Marine Geology, 49, 279-300.

Kuehl, S.A., DeMaster, D.J., Nittrouer, C.A., 1986. Nature of sediment accumulation on the Amazon continental shelf. Continental Shelf Research 6, 209-225.

Liu, K.-K., Atkinson, L., Quinones, R., Talaue-McManus, L., 2010. Carbon and Nutrient Fluxes in Continental Margins. Springer-Verlag Berlin Heidelberg.

Mayorga, E., Aufdenkampe, A.K., Masielo, C.A., Krusche, A.V., Hedges, J.I., Quay, P.D., Richey, J.E., Brown, T.A., 2005. Young organic matter as source of carbon dioxide outgassing from Amazonian rivers. Nature 436, 538-541.

McKee B.A., Aller R.C., Allison M.A., Bianchi T.S., Kineke, G.C., 2004. Transport and transformation of dissolved and particulate materials on continental margins influenced by major rivers: benthic boundary layer and seabed processes. Continental Shelf Research 24, 899–926.

Meade, R.H., Dunne, T., Richey, J.E., Santos, U.D.M., Salati, E., 1985. Storage and remobilization of suspended sediment in the lower Amazon river of Brazil. Science 228, 488-490.

Medeiros, P.M., Sikes, E.L., Thomas, B., Freeman, K.H., 2012. Flow discharge influences on input and transport of particulate and sedimentary organic carbon along a small temperate river, Geochimica Cosmochimica Acta, 77, 317–334.

Medeiros, P.M., Seidel, M., Ward, N.D., Carpenter, E.J., Gomes, H.R., Niggemann, J., Krusche, A.V., Richey, J.E., Yager, P.L., Dittmar, T., 2015. Fate of the Amazon River dissolved organic matter in the tropical Atlantic Ocean. Global Biogeochemistry Cycles 29, 677–690.

Meybeck, M., 1982. Carbon Nitrogen and Phosphorous transport by world rivers. American Journal of Science 282, 401-450.

Meziane T., Tsuchiya M., 2000. Fatty acids as tracers of organic matter in the sedimentand food web of a mangrovelintertidal flat ecosystem, Okinawa, Japan. Marine Ecology Progress Series 200, 49-57.

Molleri, G.S.F., Novo, E.M.L.M., Kampel M., 2010. Space-time variability of the Amazon River plume based on satellite ocean color. Continental Shelf Research 30, 342–352.

Molinier, M., Guyot, J.L., Oliveira E., Guimarães V., 1996. In L'hydrologie tropicale. IAHS Publ 238, 209–222.

Moreira-Turcq, P., Jouanneau, J.M., Turcq, B., Seyler, P., Weber, O., Guyot, J.L., 2004. Carbon sedimentation at Lago Grande de Curuai, a floodplain lake in the low Amazon Region: insights into sedimentation rates. Palaeogeography, Palaeoclimatology, Palaeoecology 214, 27–40.

Moreira-Turcq, P., Bonnet, M.P., Amorim, M., Bernardes, M.C., Lagane, C., Maurice, L., Perez, M., Seyler, P., 2013. Seasonal variability in concentration, composition, age and fluxes of particulate organic carbon exchanged between the floodplain and the Amazon river. Global Biogeochemical Cycles 27, 1-12.

Mortillaro, J.M., Abril, G., Moreira-Turcq, P., Sobrinho, R.L., Perez, M., Meziane, T., 2011. Fatty acid and stable isotope ($\delta^{13}C$, $\delta^{15}N$) signatures of particulate organic matter in the lower Amazon river: Seasonal contrasts and connectivity between floodplain lakes and the mainstem. Organic Geochemistry 42, 1159–1168.

Nayak A. R., Twardowski M.S., 2020. “Breaking” news for the ocean’s carbon budget. Science, 367, 6479, 738-739.

Nittrouer C.A., DeMaster D.J., 1996. The Amazon shelf setting: tropical, energético, and influentes by a large river, Continental Shelf Research. 16, 5/6, 553-573.

O’Melia, C.R., Tiller, C.L., 1993. Physicochemical aggregation and deposition in aquatic environments. In: Buffle, J., van Leeuwen, H.P. (Eds.), Environmental Particles, Vol. 2. Lewis Publishers, Boca Raton, FL, 353–386.

Prestesa, Y.O., Silva, A.C., Jeandel, C., 2018. Amazon water lenses and the influence of the North Brazil Current on the continental shelf. Continental Shelf Research 160, 36–48.

Raymond P.A., Bauer, J.E., 2001. riverine export of aged terrestrial organic matter to the north Atlantic Ocean. Nature 409, 497-500.

Pitcher, A., Hopmans, E.C., Schouten, S., Sinninghe Damsté, J.S., 2009. Separation of core and intact polar archaeal tetraether lipids using silica columms: Insights into living and fossil biomass contributions. Organic Geochemistry 40, 12-19.

Richey, J.E., Hedges, J.I., Devol A.H., Quay, P.D., Victoria R., Martinelli, L., Forsberg, B.R., 1990. Biogeochemistry of carbon in the Amazon river. Limnology and Oceanography 35, 352-371.

Scheufuß, E., Ratmeyer, V., Stuut, J-B.W., Jansen, J.H.F., Sinninghe Damsté, J.S., 2003. Carbon isotope analyses of n-alkanes in dust from the lower atmosphere over the central eastern Atlantic. Geochimica et Cosmochimica Acta. 67, 1757–1767.

Schlünz, B., Schneider, R.R., 2000. Transport of terrestrial organic carbon to the oceans by rivers: re-estimating flux- and burial rates. International Journal of Earth Sciences 88, 599-606.

Schouten, S., C. Huguet, E. C. Hopmans, M. V. M. Kienhuis, and J. S. Sinninghe Damsté. 2007. Improved analytical methodology for TEX86 paleothermometry by high performance liquid chromatography/atmospheric pressure chemical ionization-mass spectrometry. Anal. Chem. 79:2940–2944.

Schouten, S., Hopmans, E.C., Baas, M., Boumann, H., Standfest, S., Könneke, M., Stahl, D.A., Sinninghe Damsté, J.S., 2008. Intact membrane lipids of "Candidatus Nitrosopumilus maritimus," a cultivated representative of the cosmopolitan mesophilic Group I Crenarchaeota. Applied and Environmental Microbiology 74, 2433-2440.

Schouten, S., Hopmans, E.C., Damsté, J.S.S., 2013. The organic geochemistry of glycerol dialkyl glycerol tetraether lipids: A review. Organic Geochemistry 54, 19–61

Seidel, M., Yager, P.L., Ward, N.D., Carpenter, E.J., Gomes, H.R., Krusche, A.V., Richey, J.E., Dittmar, T., Medeiros, P.M., 2015. Molecular-level changes of dissolved organic matter along the Amazon River-to-ocean continuum. Marine Chemistry. 177, 218–231.

Showers, W.J., Angle, D.G., 1986. Stable isotopic characterization of organic carbon accumulation on the Amazon continental shelf. Continental Shelf Research 6, 227-244.

Singh, M., Singh, I.B., Müller, G., 2007. Sediment characteristics and transportation dynamics of the Ganga river. Geomorphology 86, 144-175.

Sinninghe Damsté, J.S., 2016. Spatial heterogeneity of sources of branched tetraethers in shelf systems: The geochemistry of tetraethers in the Berau river delta (Kalimantan, Indonesia). Geochimica et Cosmochimica Acta 186, 13-31.

Smith Jr, W.O., Demaster, D.J., 1996. Phytoplankton biomass and productivity in the Amazon river plume: correlation with seasonal river discharge. Continental shelf research. 16, 291-319.

Smith, R.W., Bianchi, T.S., Savage, C., 2010. Comparison of lignin phenols and branched/isoprenoid tetraethers (BIT index) as indices of terrestrial organic matter in Doubtful Sound, Fiordland, New Zealand. Organic Geochemistry 41, 281-290.

Sun, S., Schefuß, E., Mulitza, S., Chiessi, C.M., Sawakuchi, A.O., Zabel, M., Baker, P.A., Hefter, J., Mollenhauer, G., 2017. Origin and processing of terrestrial organic carbon in the Amazon system: lignin phenols in river, shelf, and fan sediments. Biogeosciences, 14, 2495–2512.

Walker, N.D., Hammack, A.B., 2000. Impacts of winter storms on circulation and sediment transport: Atchafalaya– Verilion Bay Region, Louisiana, USA. Journal of Coastal Research 16, 996–1010.

Ward, N.D., Keil, R.G., Medeiros, P.M., Brito, D.C., Cunha, A.C., Dittmar, T., Yager, P.L., Krusche, A.V., Richey, J.E., 2013. Degradation of terrestrially derived macromolecules in the Amazon river. Nature Geoscience 6, 530-533.

Ward, N.D., Krusche, A.V., Sawakuchi, H.O., Brito, D.C., Cunha, A.C., Moura, J.M.S., Silva, R., Yager, P.L., Keil, R.G., Richey, J.E., 2015. The compositional evolution of

dissolved and particulate organic matter along the lower Amazon River—Óbidos to the ocean. Marine Chemistry. 177, 244256.

Weijers, J.W.H., Schouten, S., Schefuß, E., Schneider, R.R., Sinninghe Damsté, J.S., 2009. Disentangling marine, soil and plant organic carbon contributions to continental margin sediments: A multi-proxy approach in a 20,000-year sediment record from the Congo deep-sea fan. Geochimica et Cosmochimica Acta 73, 119-132.

Whitehouse, U.G., Jeffrey, L.M., DeBrecht, J.D., 1960. Differential settling tendencies of clay minerals in saline waters. In: Swineford, A., (Ed.), Clays and Clay Minerals, Proceedings of the Seventh National Conference, 1–79.

Wright, L.D., Yang, Z.-S., Bornhold, B.D., Keller, G.H., Prior, D.B., Wiseman Jr., W.J., 1986. Hyperpycnal plumes and plume fronts over the Huanghe (Yellow River) delta front. Geo-Marine Letters 6, 97–105.

Zell, C., Kim, J.-H., Moreira-Turcq, P., Abril, G.l., Hopmans, E.C., Bonnet, M.-P., Sobrinho, R.L., Sinninghe Damsté, J.S., 2013a. Disentangling the origins of branched tetraether lipids and crenarchaeol in the lower Amazon river: Implications for GDGT-based proxies. Limnology and Oceanography. 58, 343-353.

Zell, C., Kim, J.-H., Abril, G., Sobrinho, R.L., Dorhout, D., Moreira-Turcq, P., Sinninghe Damsté, J.S., 2013b. Impact of seasonal hydrological variation on the distributions of tetraether lipids along the Amazon river in the central Amazon basin: implications for the MBT/CBTpaleothermometer and the BIT index. Frontiers in Microbiology 24, 1-14.

Zhu, C., Wagner, T., Talbot, H.M., Weijers, J.W.H., Pan, J.-M., Pancost, R.D., 2013. Mechanistic controls on diverse fates of terrestrial organic components in the East China Sea. Geochimica et Cosmochimica Acta 117, 129-143.

Figure captions

Figure 1 – Map showing the stations in the Amazon continental shelf area and southern North Atlantic. Roman numbers represent the four regions defined in this study (see text).

Figure 2 – TOC content (A), bulk $\delta^{13}C$ content (B), concentration of brGDGTs (C), concentration of crenarchaeol (D), estimations of BIT index (E), concentration of λ8 (F), concentration of total fatty acids content (G), concentration of long chain fatty acids (L.C.F.A.) (H), concentration of $C_{27\text{-}33}$ *n*-alkanes (I) for each station.

Figure 3 – Results of the estimations for OC_{cont} based on bulk organic carbon, lignin phenols and GDGTs for each station (A). Roman numbers represent the four regions approached in this study. Box plot represent the mean values for the estimations of OC_{cont} in each region (B).

Figure 4 - Box plots showing the results of Equation 5. The mean values represent the ΔOC_{cont} calculated for each biomarker taking into account all the sediment samples analyzed.

Figure 5 – Bar plots show the accumulation rate (AR) based on bulk organic carbon, lignin phenols and GDGTs for each station approached in this study.

Figure 6 – Spatial distribution of the average values for the estimations of AR_{OC} based on bulk organic carbon, lignin phenols and GDGTs in each sampling site. The diameter of each circle is proportional to the estimations of AR_{TOC} ($g_{OC}\ m^{-2}\ y^{-1}$) as estimated by Equation 6.

Table 1: Results of bulk parameters and biomarkers in surface sediments of the Amazon continental shelf.

					F.A. (mg g_{oc}^{-1})			*n*-alkanes (mg g_{oc}^{-1})		GDGT$_{CL}$ (µg g_{OC}^{-1})			Lignin Phenols (mg g_{OC}^{-1})						
Region	Sample	Deph (m)	TOC (wt%)	$\delta^{13}C$ (‰)	$\sum_{Total}$	LCFA (≥24:0)	Even:Odd (20:0-30:0)	C_{27-33} (Odd)	CPI	brGDGTs	crenarchaeol	BIT-Index	Λ8	S	V	C	S:V	C:V	(Ad:Al)v
I	ANC-14	28	0.05	-19.8	6.1	1.3	4.4	0.7	1.6	13.3	159.6	0.08	1.8	0.8	1.0	0.03	0.82	0.03	0.20
	ANC-13	23	0.03	-25.3	5.5	1.5	3.7	0.5	1.5	14.0	29.2	0.32	5.0	1.8	3.0	0.10	0.60	0.03	0.24
II	ANC-10	14	0.58	-26.8	4.2	1.9	2.8	0.3	1.9	56.6	42.1	0.57	41.2	15.4	24.8	0.88	0.62	0.04	0.18
	ANC-11	16	0.86	-27.3	3.2	2.0	1.3	0.4	2.3	31.1	28.7	0.52	13.3	5.3	7.6	0.44	0.70	0.06	0.29
III	ANC-5	66	1.11	-21.1	1.9	0.6	3.4	0.2	2.1	7.9	94.4	0.08	0.7	0.2	0.4	0.03	0.55	0.07	0.25
	ANC-16	433	0.16	-21.9	4.2	0.7	3.5	0.2	2.0	15.6	126.6	0.11	3.5	1.4	2.1	0.07	0.66	0.03	0.27
IV	ANC-2	4269	0.88	-20.7	0.9	0.4	3.0	0.1	2.4	5.7	104.3	0.05	0.2	0.0	0.2	0.02	0.32	0.14	0.19
	ANC-1	4299	0.82	-20.3	1.1	0.3	2.9	0.1	2.2	3.9	60.0	0.06	0.2	0.1	0.1	0.03	0.43	0.24	0.13

Table 2: Parameters related to the discharge, primary production and sedimentation of organic matter in the Amazon continental shelf used in this study. End-member values for $\delta^{13}C$, BIT Index and ʎ8 in the SPOM are applied in the mixing model approach (see text). The values were found in the literature, as presented.

Parameter	Average Value	Reference
Particule density	2.75 g cm^{-3}	Kuehl et al. (1982)
Porosity	75% (Regions I, II, III) 93% (Region IV)	Kuehl et al. (1982) Chong et al.(2014)
Deposition Rate (DR)	0.5 cm y^{-1} (Region I,II) 0.25 cm y^{-1} (Region III) 0.1 cm y^{-1} (Region IV)	Chong et al. (2014); Showers and Angle (1986)
$\delta^{13}C$ (SPOM): Amazon River \ Marine	-29.7 (‰)\ -20.0 (‰)	Burdige (2005); Mayorga et al. (2005)
BIT-Index (SPOM): Amazon river \ Marine	0.7 ± 0.2 \ 0.04 ± 0.02	Schouten et al. (2013); Zell et al. (2013b)
λ8 (SPOM): Amazon River	18 mg g_{OC-1}	Ward et al. (2015)

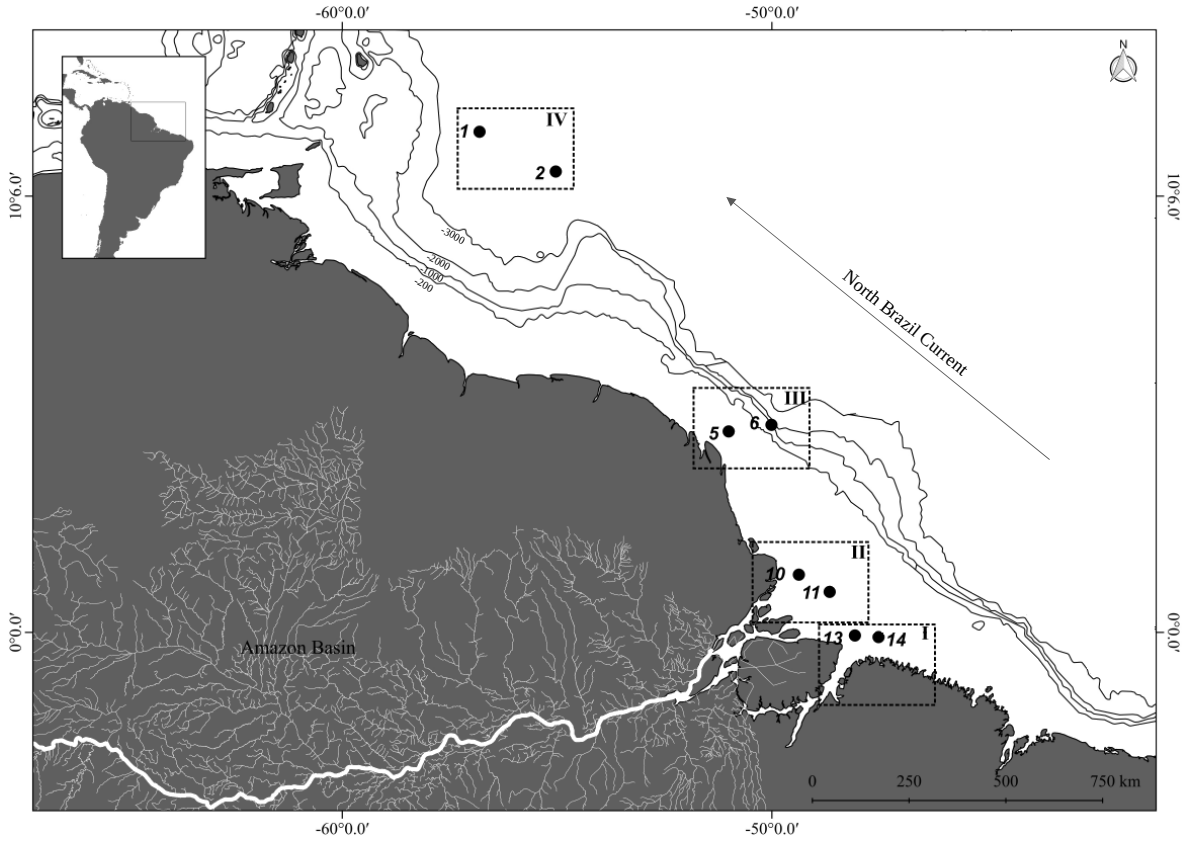
-60°0.0′
-50°0.0′
10°6.0′
0°0.0′
N
IV
1
2
III
5
6
II
10
11
I
13
14
-3000
-2000
-1000
-200
North Brazil Current
Amazon Basin
0
250
500
750 km

Figure 1

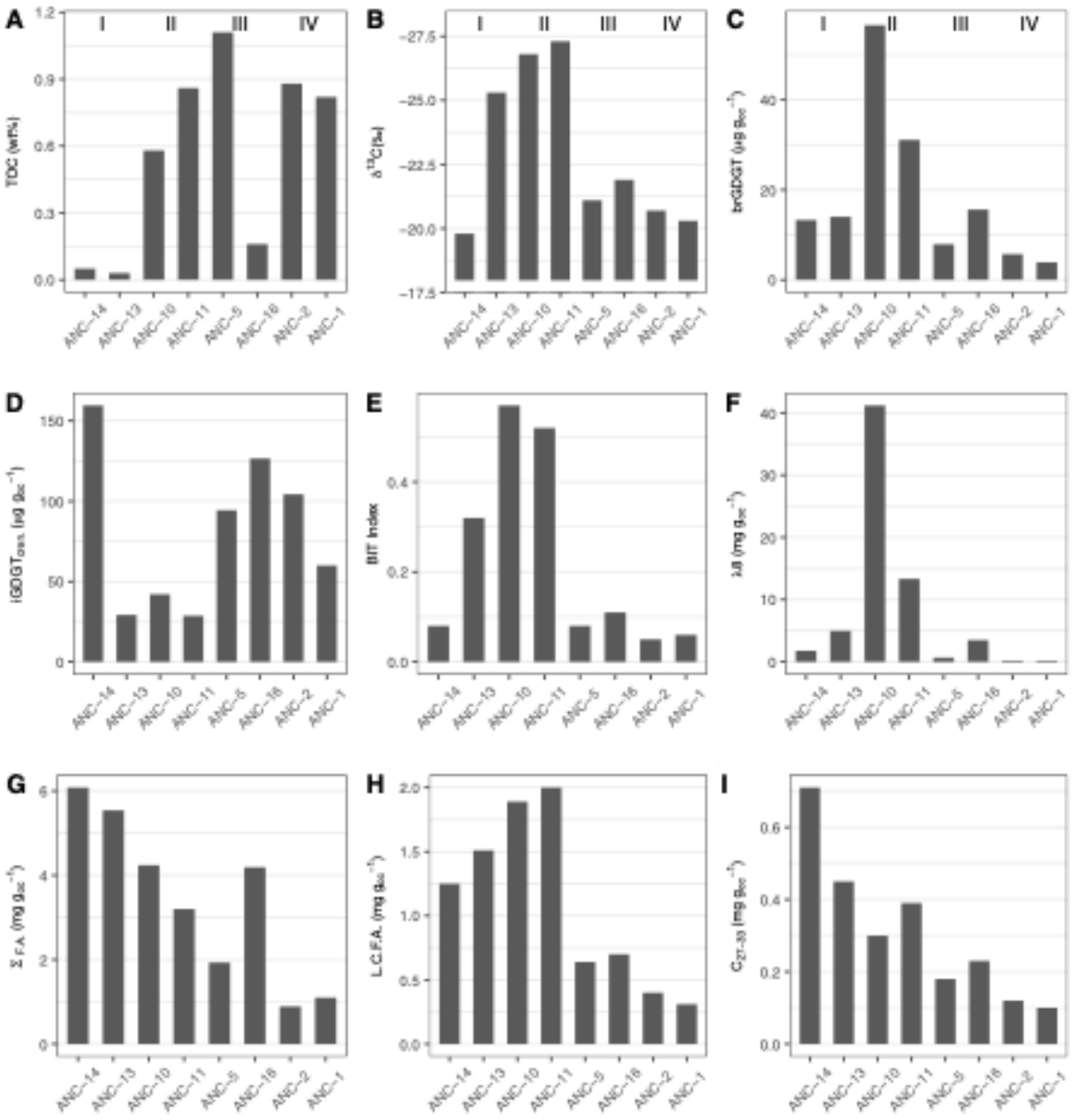
A
B
C
D
E
F
G
H
I
I
II
III
IV
TOC (wt%)
δ13C (‰)
brGDGT (µg gdw−1)
iGDGTOxic (ng gdw−1)
BIT Index
iA (mg gdw−1)
Σ F.A. (mg gdw−1)
L.C.F.A. (mg gdw−1)
C27-33 (mg gdw−1)
ANC−14
ANC−13
ANC−10
ANC−11
ANC−5
ANC−16
ANC−2
ANC−1

Figure 2

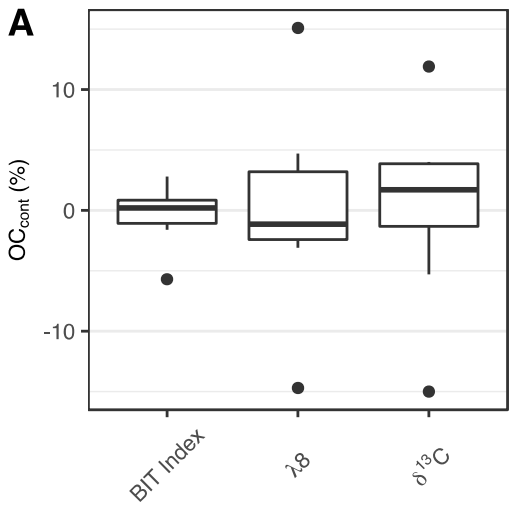

Figure 3

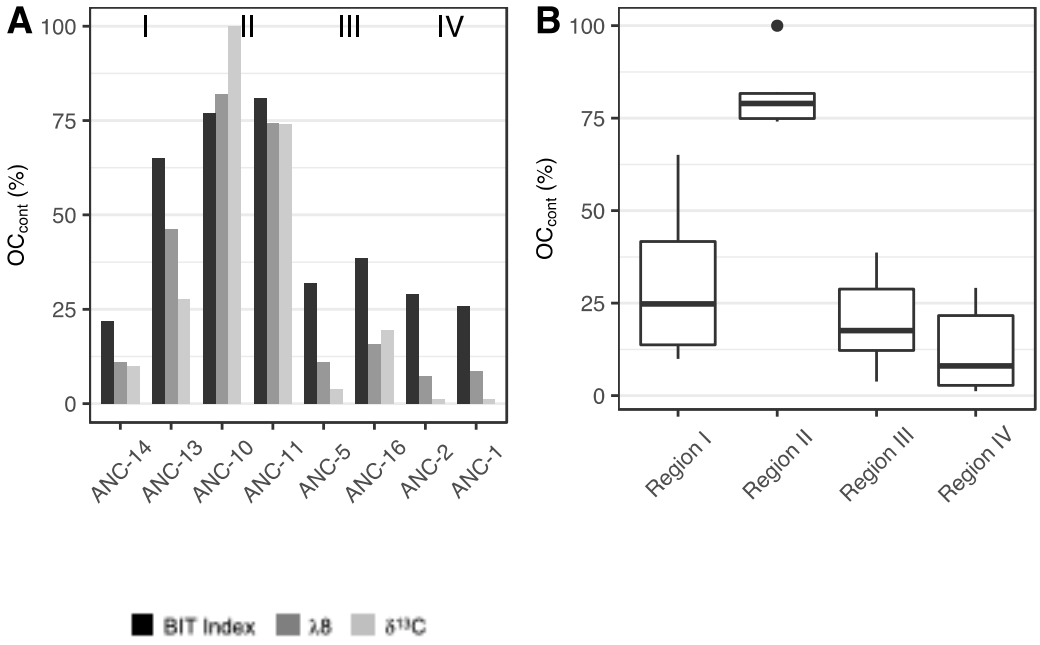
A
B
I
II
III
IV
100
75
50
25
0
OC$_{cont}$ (%)
ANC-14
ANC-13
ANC-10
ANC-11
ANC-5
ANC-16
ANC-2
ANC-1
Region I
Region II
Region III
Region IV
BIT Index
λ,8
δ^{13}C

Figure 4

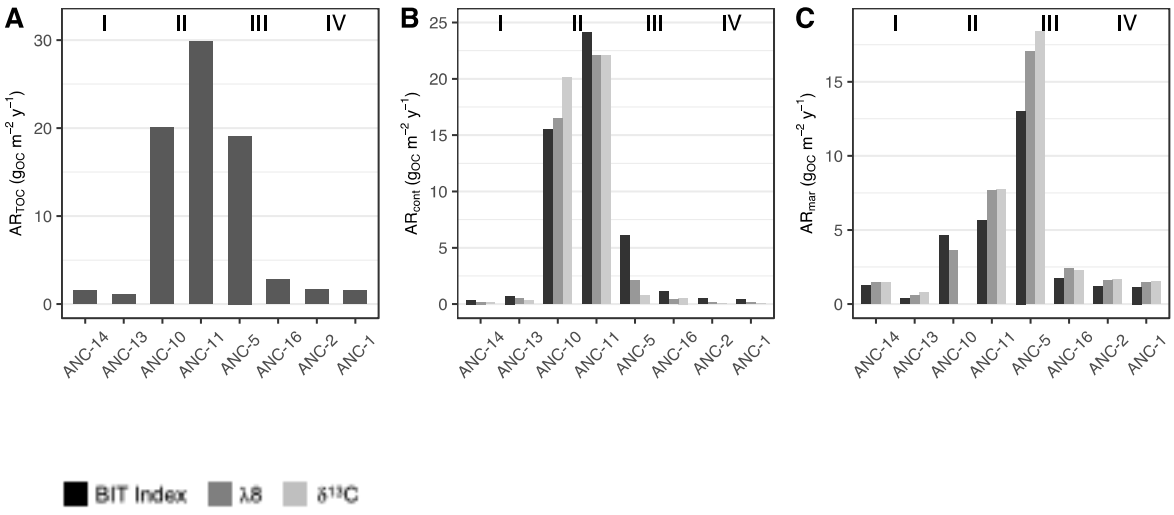
A
B
C
I
II
III
IV
ANC-14
ANC-13
ANC-10
ANC-11
ANC-5
ANC-16
ANC-2
ANC-1
BIT Index
λ8
δ13C

Figure 5

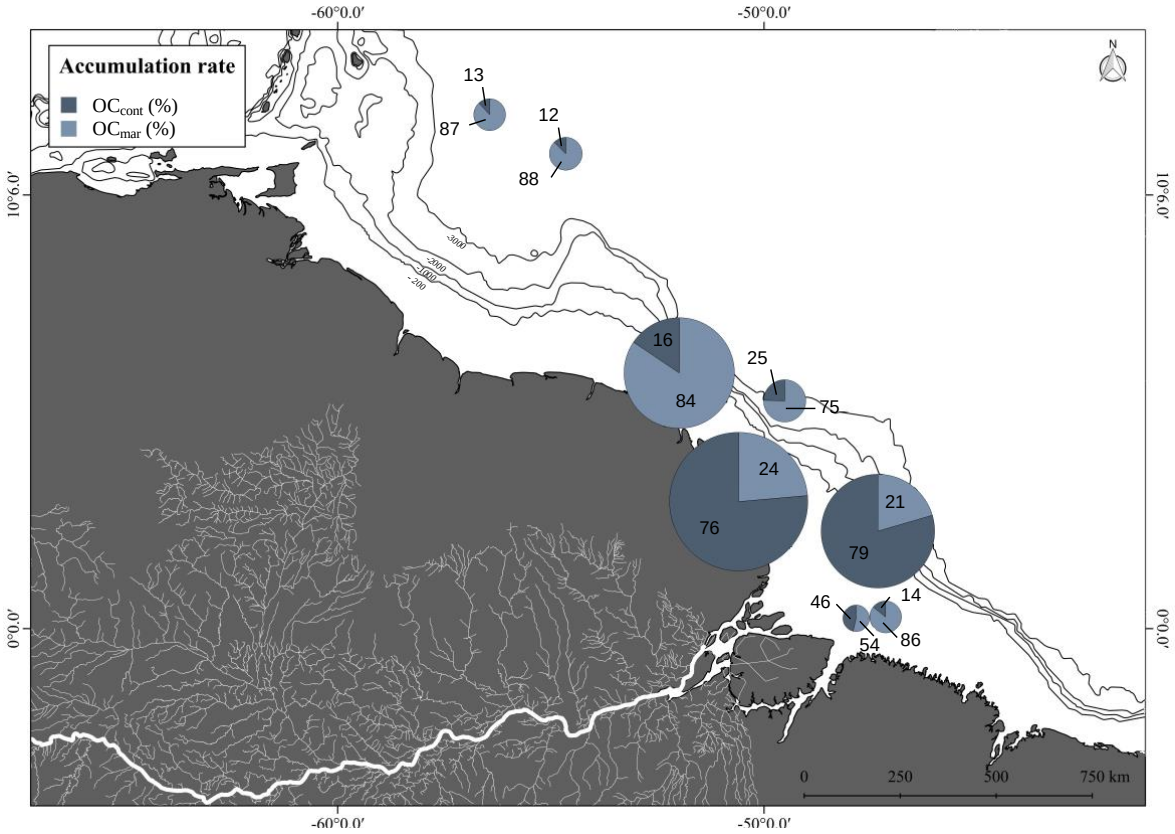
Accumulation rate
OC$_{cont}$ (%)
OC$_{mar}$ (%)
-60°0.0′
-50°0.0′
10°6.0′
0°0.0′
N
13
87
12
88
16
84
25
75
24
76
21
79
46
54
14
86
-3000
-2000
-1000
-200
0
250
500
750 km

Figure 6